THE JOURNAL OF PHYSICAL CHEMISTRY B

Article

pubs.acs.org/JPCB

Electron Attachment to the Cytosine-Centered DNA Single Strands: Does Base Stacking Matter?

Jiande Gu,*[,†] Jing Wang,[‡] and Jerzy Leszczynski*[,‡]

[†]Drug Design & Discovery Center, State Key Laboratory of Drug Research, Shanghai Institute of Materia Medica, Shanghai Institutes for Biological Sciences, CAS, Shanghai 201203, P. R. China

[‡]Interdisciplinary Nanotoxicity Center, Department of Chemistry, Jackson State University, Jackson, Mississippi 39217, United States

Supporting Information

ABSTRACT: Electron attachment to the trimer of nucleotide, dGpdCpdG, has been investigated by a quantum mechanical approach at a reliable level of theory. The study of the electron attached dGpdCpdG species demonstrates that cytosine contained DNA single strands have a strong tendency to capture low-energy electrons and to form electronically stable cytosine-centered radical anions. The comparative study of the model molecules pdCpdG and dGpdCp reveals that base stacking has little contribution to the adiabatic electron affinity (AEA) of cytosine in DNA single strands. Additionally, the base−base stacking does not affect the vertical detachment energy (VDE) of the cytosine-centered radicals. Intrastrand H-bonding is found to be critical in increasing the values of the AEA and VDE. However, base−base stacking is revealed to be important in enlarging the vertical electron affinity (VEA) of cytosine. The electron attachment to the cytosine moiety intensifies the intrastrand H-bonding between the neighboring G and C bases. This process disrupts the base−base stacking interaction in the radical anion of dGpdCpdG.

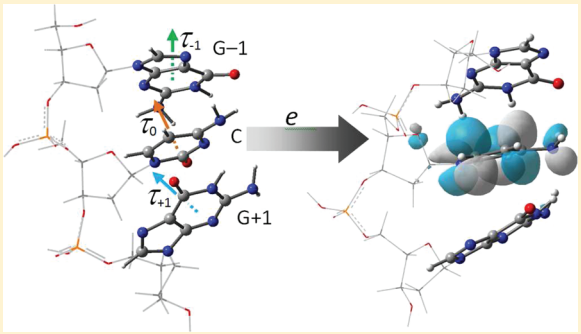

I. INTRODUCTION

Electron attachment to DNA and RNA fragments represents an important factor that could lead to understanding the mechanism of DNA and RNA chemical reactions.[1−5] This process has been found to play an important role in biochemical processes related to DNA damage and repair,[1,6−12] charge transfer along DNA,[13−17] and the initiation of reactions leading to mutation.[16,18] Comprehension of the details of the electron attachment to DNA and RNA requires explicit interactions among various biological and chemical disciplines. Due to improvements in both experimental techniques and theoretical methods, the investigation of the electron attachment to DNA, RNA, and their subunits has been greatly advanced since 1990.

An application of the extrapolating methods for experiments with microsolvated nucleobases revealed that the pyrimidines have near-zero electron affinities (EAs).[19,20] Experimental studies in the gas phase have resulted in negative EA values for adenine (A) and cytosine (C).[21−24] Recent photoelectron spectroscopic experiments (along with theoretical calculations) have detected anionic states of tautomers of adenine and guanine (G) which exhibit relatively large vertical electron detachment energies (VDEs).[24,25] Electron attachment to nucleosides has been studied experimentally by Bowen's group.[26] The experimental values[26] of the electron affinities of thymidine, cytidine, and adenosine are within 0.2 eV of the theoretical predictions reported earlier.[3] Beyond nucleosides, experiments on the electron-capturing abilities of short DNA oligomers are able to provide estimates of the relative order of the vertical attachment energies (VAEs) for DNA single strands, while no direct determinations of the electron affinities have been reported.[2] On the other hand, the photoelectron spectra of the anionic base pairs of adenine and thymine (AT^-) and 9-methyladenine and 1-methylthymine ($mAmT^-$) recorded the large VDE (0.7−1.7 eV) for these radical anions of the base pairs in the tautomeric forms.[27,28]

Parallel to experimental studies, theoretical investigations at various levels of complexity have complemented the exploration of the electron attachment to DNA and RNA. The coupled cluster level of theory with single, double, and perturbative triple excitations (CCSD(T)) study revealed the details of tautomeric forms related to covalently bound radical anions of guanine[25,29] and adenine. This study successfully elucidated the experimental observations.[24] Reliable experimental AEA values of individual nucleic acid bases have been reproduced by the advanced density functional theory (DFT) approaches.[30−32] Gradually, with the extensively calibrated B3LYP/DZP++ approach,[33] a reliable data bank of the electron affinities of the 2′-deoxyribonucleosides,[3] the nucleotides (3′-dCMP, 3′-dTMP, 5′-dCMP, 5′-dTMP),[1,4,34,35] and the nucleoside-3′,5′-diphosphates (3′,5′-dGDP, 3′,5′-dADP, 3′,5′-dCDP, and 3′,5′-dTDP)[5] has been established. The predicted values of AEA and

Received: November 26, 2011
Revised: December 24, 2011
Published: January 8, 2012

ACS Publications © 2012 American Chemical Society

dx.doi.org/10.1021/jp211386x | J. Phys. Chem. B 2012, 116, 1458−1466

Scheme 1. Models of DNA Single Strand: Trinucleoside Phosphate (dGpdCpdG) and Dinucleoside Phosphates (dGpdCp and pdCpdG)[a]

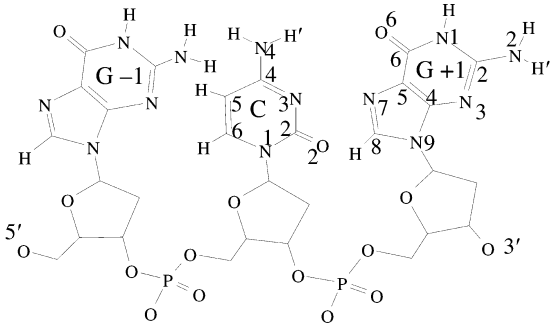

dGpdCpdG

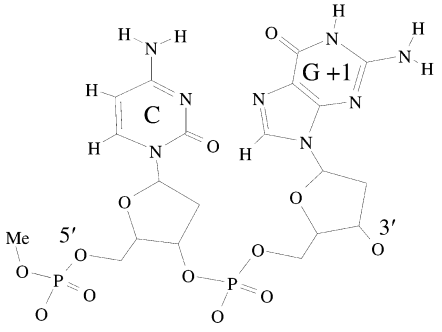

pdCpdG

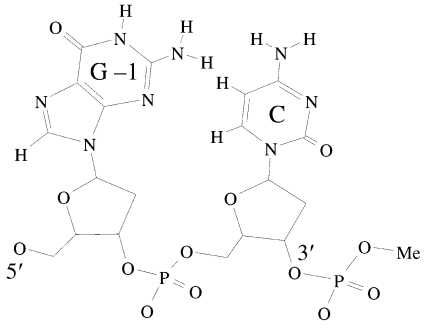

dGpdCp

[a]To mimic the oligomer of DNA single strand, a methyl group is used to replace one of the protons in the phosphate at the end position of the dimers of the nucleotide. Hydrogen atoms attached to the ribose-phosphate backbones have been omitted for clarity.

VDEs of the nucleosides have been confirmed later by the photoelectron spectroscopic experiments.[26] As a crucial step to achieve the realistic description of electron attachment to the single-strand nucleotide oligomers, the dinucleoside phosphate deoxycytidylyl-3′,5′-deoxyguanosine (dCpdG), dinucleoside phosphate deoxyguanylyl-3′,5′-deoxycytidine (dGpdC),[36] dinucleoside phosphate deoxythytidylyl-3′,5′-deoxyadenosine (dTpdA), and dinucleoside phosphate deoxyadenylyl-3′,5′-deoxythytidine (dApdT),[37] and the corresponding radical anions, have been investigated recently using the reliable DFT approaches.

Theoretical studies have been extended to explore the electron attachment to the hydrogen-bonding paired DNA subunits, including nucleobase pairs,[27,38−41] the nucleoside pairs,[42,43] and nucleotide−nucleobase pairs.[44] Computational methods have been applied to elucidate the electron capture abilities of the A:T pair and mA:mT pair in their tautomeric forms.[27] The electron affinities of thymine-adenine base-pair stacking between different bases were studied by the resolution of identity MP2 (RI-MP2) approach.[45] The influences of microhydration on the electron attachment to nucleobases have also been investigated extensively at different levels of theory.[46−59] Recently, the electron affinities of the hydrated double helix of dinucleoside phosphate deoxyguanylyl-3′,5′-deoxycytidine have been predicted on the basis of the density functional theory.[60]

To approach a realistic description of DNA, one should include the most important stabilization factors such as base−base, base−backbone, and hydration interactions in the model system. Previous studies of the minimal segments of the DNA single strands (dTpdA and dApdT)[37] and double-helical complex dGpdC dimer octahydrate[60] contain all of these most crucial stabilization factors. However, the methods used in those studies do not accurately describe one of the most important interactions in the system, i.e., the base−base stacking interaction. Although the study of the hydrated dGpdC and dCpdG complexes with the BH&H and M05-2X functionals (which do describe the base−base stacking properly) suggests that the stacking interaction does not improve the electron capture ability of C in the system, the role of the electron attachment in the base−base stacking of DNA has not been fully addressed.[36] Furthermore, to understand the electron attachment to the cytosine in the single-strand DNA, one needs to consider a more rational situation in which C is sandwiched between two neighboring bases.

Here we report our recent developments in theoretical studies of the electron attachment to DNA single-strands. The trimer of deoxynucleoside phosphate dGpdCpdG (see Scheme 1) has been adopted to model the cytosine in the guanine rich DNA strands. Previous studies of the electron attachment to the dimers of dGpdC and dCpdG reported the corresponding electron affinities to be 0.66 eV for dGpdC and 0.90 eV for dCpdG.[36] The position of cytosine in the oligomer affects the electron capture capability of cytosine. The cytosine in these models is at the terminal positions. Selection for this study of dGpdCpdG which holds the cytosine inside the DNA strands represents a logical augmentation of the previous models. In order to examine the influence of the base−base stacking

dx.doi.org/10.1021/jp211386x | J. Phys. Chem. B 2012, 116, 1458−1466

interactions on the electron attachment, two more model complexes dGpdCp and pdCpdG are also considered in this study. Investigation of these model complexes is able to provide details of electron attachment to the cytosine site in DNA single strands. It should be noted that the phosphate group in the model is not deprotonated in the gas phase. Although deprotonation is expected in aqueous solutions, studies by Schaefer's group indicate that the electron affinities corresponding to formation of the base-centered radical anions of nucleotides are independent of the existence of counterions in aqueous solutions.[61] Therefore, the deprotonated phosphate model will not be considered in this study.

II. THEORETICAL METHODS

Although the calibrated DFT approach[33] B3LYP[62,63]/DZP++ predicted effectively electron affinities for all of the DNA and RNA subunits, it is not the best computational model for the considered systems in which base−base stacking governs the structural characteristics. The successful application of the B3LYP/DZP++ method in the previous studies of electron attachment to the nucleotide oligomers dCpdG, dGpdC, dApdT, and dTpdA is based on the fact that the hydration water molecules in the investigated systems "lock" bases in the stacking pattern through H-bonding.[36,37] On the other hand, the density functional M05-2X,[64,65] which is able to model the stacking interaction properly, provides the electron affinities of the hydrated dCpdG and dGpdC close to that predicted by the B3LYP method.[36] A recent study reveals that the M05-2X method is suitable to describe three stacked layer systems such as dGpdCpdG.[66] Therefore, the M05-2X functional along with the basis set DZP++ was adopted in the present study. The selection of the DZP++ basis set is aiming to keep the consistency with the previous studies of the electron attachment to DNA fragments. The DZP++ basis sets were constructed by augmenting the Huzinaga−Dunning[67,68] set of contracted double-ζ Gaussian functions with one set of p-type polarization functions along with one even-tempered diffuse s function for each H atom and one set of five d-type polarization functions in addition to sets of even-tempered diffuse s and p functions for each C, N, O, and P atom. The even-tempered orbital exponents were determined according to the prescription of Lee.[69] Adiabatic electron affinity was computed as the difference between the absolute energies of the appropriate neutral and anion species at their respective optimized geometries, AEA = $E_{neut} - E_{anion}$. Following the previous studies,[4,5,34,36] in the present study, singlet spin states were assumed for the neutral systems and doublet spin states were assumed for the corresponding radical anions.

To analyze the distributions of each unpaired electron, the molecular orbital and the spin density plots were constructed from the corresponding M05-2X/DZP++ densities. Natural population analysis (NPA) was carried out using the natural bond orbital (NBO) method of Reed and Weinhold.[70,71] The Barone−Tomasi polarizable continuum model (PCM)[72] with the standard dielectric constant of water (ε = 78.39) was used to simulate the solvated environment of an aqueous solution. The Gaussian 03 system of DFT programs[73] was used for all computations.

III. RESULTS AND DISCUSSION

A. Geometries. *dGpdCpdG.* The fully optimized geometry of the neutral dGpdCpdG is depicted in Figure 1, and the

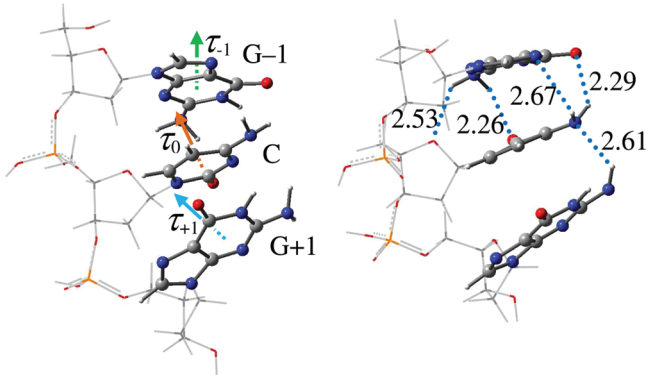

Figure 1. Two views of the optimized geometrical structure for the neutral dGpdCpdG. Atomic distances are in Å. Color representations: orange for P, gray for C, red for O, blue for N, and white for H. τ_0 is the vector of the plane defined by N1C5N3 of C, τ_{-1} is the vector of the plane defined by N1N3C5 of G−1, and τ_{+1} is the vector of the plane defined by N1N3C5 of G+1.

geometric parameters of the base−base interaction pattern are summarized in Table 1. The base−base distances (3.27 and 3.37 Å) and the angles between the base-planes (12.9 and 15.0°) exhibit the typical geometric characteristics of the stacked bases (2.3−3.4 Å for base−base distance and 1−19° for base inclination to the axis).[74] Besides the base−base stacking interaction, H-bonding between the bases can be seen from the revealed structural parameters. The atomic distance (2.29 Å) between O6(G−1) and H4(C) and the atomic angle (134.9°) among O6(G−1)H4N4(C) in dGpdCpdG suggest the H-bonding interaction through O6(G−1) and H4(C). The atomic distance of 2.26 Å for H2(G−1) and O2(C) and the atomic angle of 127.3° for N2H2(G−1)O2(C) indicate existence of another H-bond between the G−1 and C bases. Moreover, a weak H-bond can be assigned to the H′2 of G−1 and the O4′ of the ribose linked to cytosine (the H′2(G−1)···O4′(C) distance is 2.53 Å, and the bond angle is 133.9°). To verify that H′2(G−1)···O4′(C) represents the H-bond, electron density difference analysis was performed on the basis of the electron density of dGpdCpdG and that of the separated nucleotides dGp, pdCp, and pdG. The electron density difference map depicted in Figure 2 reveals the electron density increase (up to 0.01 au) between H′2(G−1) and O4′(C). This electron density boost confirms the H-bonding interaction between these two atoms.[75,76] The existence of these H-bonds between C and G−1 is in accordance with their base−base distance (3.27 Å).

In general, the electron attachment to dGpdCpdG increases the H-bonding interaction between the bases. Specifically, the H2(G−1)···O2(C) and H′2(G−1)···O4′(C) bond lengths amount to 2.07 and 2.14 Å, respectively, in the radical anion of dGpdCpdG (Figure 3). Compared to the neutral species, these two H-bonds reduce their bond lengths by 0.19 Å for the former and 0.39 Å for the latter. However, the O6(G−1)···H4(C) H-bond length increases to 2.36 Å in dGpdCpdG$^{\bullet-}$, about 0.07 Å longer than that in the neutral compound. Furthermore, an H-bond can also be found between C and G+1. The atomic distance of 2.21 Å (which amounts to 2.61 Å in the neutral species) between H2(G+1) and N4(C) indicates existence of a H-bond of moderate strength. Notice that for the H-bonds H2(G−1)···O2(C), H′2(G−1)···O4′(C), and H2(G+1)···N4(C) the cytidine moiety represents the proton acceptor, while for the H-bond O6(G−1)···H4(C) cytosine is

dx.doi.org/10.1021/jp211386x | J. Phys. Chem. B 2012, 116, 1458−1466

Table 1. Base−Base Stacking Parameters of the Models dGpdCpdG, pdCpdG, dGpdCp, and Their Corresponding Radical Anions (the Base−Plane Distance (in Å) and Angle (in deg) of the Base-Planes between the Bases)[a]

species	dGpdCpdG	dGpdCpdG$^{\bullet-}$	pdCpdG	pdCpdG$^{\bullet-}$	dGpdCp	dGpdCp$^{\bullet-}$
R_{CG-1}	3.268	3.240			3.208(3.36)	3.461(3.35)
R_{CG+1}	3.369	3.282	3.493(3.53)	3.786(3.48)		
θ_{CG-1}	12.9°	23.1°			10.5°(10.9°)	23.8°(29.7°)
θ_{CG+1}	15.0°	16.4°	22.7°(22.5°)	38.1°(25.9°)		

[a]Base−plane distance is defined as the distance between the geometrical center formed by the N1N3C5 fragments of guanines and the base-plane formed by the N3N1C5 group of cytosine. The angle between base-planes is defined as the angle between the vector determined by N1N3C5 of cytosine (τ_0, see Figure 1) and the vector determined by N1N3C5 of guanines. Numbers in parentheses are from ref 36, in which the models used were tetra-hydrated dGpdC and tetra-hydrated dCpdG.

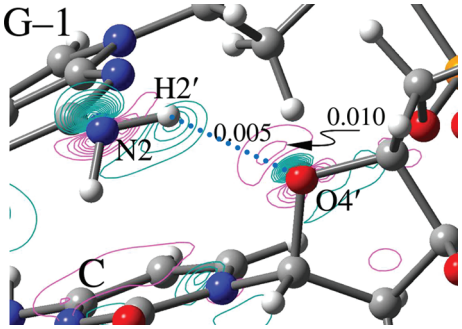

Figure 2. The iso-value contour map of the electron density difference (on the plane defined by N2H2′O4′) around the H-bond H′2(G−1)···O4′(C) moiety. Pink stands for the positive and blue for negative values. Unit is in au.

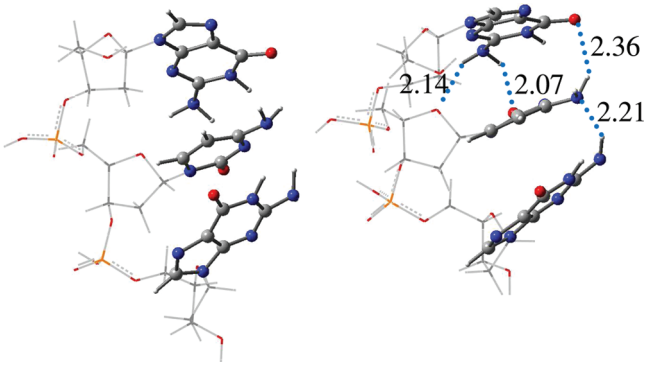

Figure 3. Two views of the optimized geometrical structure for the radical anion of dGpdCpdG. Atomic distances are in Å. Color representations: orange for P, gray for C, red for O, blue for N, and white for H. The guanine at the top layer is denoted as G−1, and the guanine at the bottom layer, as G+1.

the proton donor. The significant reinforcement of the proton accepting capability of cytosine suggests that the extra electron in dGpdCpdG$^{\bullet-}$ should be located on C. Consequently, an electron attached to the cytosine slightly disrupts the base−base stacking interaction in the radical anion of dGpdCpdG. Compared to the neutral complex, the base−base distance is reduced by only about 0.03−0.09 Å due to the electron attachment. However, the effect of the electron attachment is pronounced on the mutual orientation of the bases. It results in the increase of the angle between base-planes of G−1 and C by about 10.2° (23.1° vs 12.9°) and that of G+1 and C by about 1.4° (16.4° vs 15.0°). The alteration in the base stacking parameters should be attributed to the intensified H-bonding between the bases.

pdCpdG. To examine the influence of G−1 on the electron affinities of the system, guanosine at the 5′ end of dGpdCpdG is replaced by a methyl group in this model. The optimized structure of the pdCpdG neutral compound depicted in Figure 4 suggests that C and G+1 are weakly stacked. Although the base−base distance of 3.49 Å follows a typical base stacking range, the base−base plane angle is relatively large, 22.7°. In contrast to dGpdCpdG, in which no H-bonding is detected between C and G+1 in the neutral species, there is a H-bond in pdCpdG. The atomic distance between N4(C) and H2(G+1) amounts to 2.25 Å, and the atomic angle of N4(C)H2N2(G+1) is 136.2°. The comparatively large base−base angle in pdCpdG could be attributed to the existence of this intrastrand base−base H-bonding.

The intrastrand H-bond H2(G+1)···N3(C) interaction is intensified in the radical anion of pdCpdG. Due to the electron attachment to the compound, the bond length of H2(G+1)···N3(C) decreases to 1.96 Å, about 0.29 Å shorter than that in the neutral molecule. Moreover, one more H-bond between G+1 and C, H1(G+1)···N4(C), can be identified in pdCpdG$^{\bullet-}$. The H1(G+1)···N4(C) bond length of 2.06 Å and

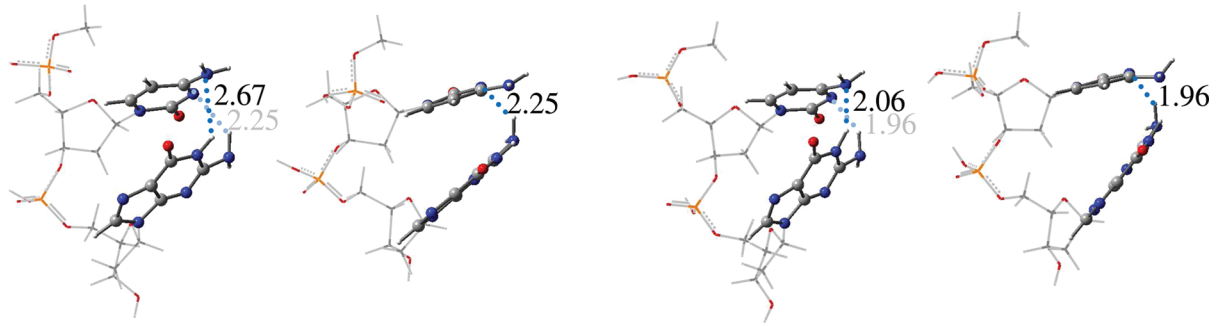

Figure 4. Two views of the optimized geometrical structures for pdCpdG and pdCpdG$^{\bullet-}$. Atomic distances are in Å. Color representations: orange for P, gray for C, red for O, blue for N, and white for H. Guanine in this dinucleoside corresponds to G+1 in dGpdCpdG.

dx.doi.org/10.1021/jp211386x | J. Phys. Chem. B 2012, 116, 1458−1466

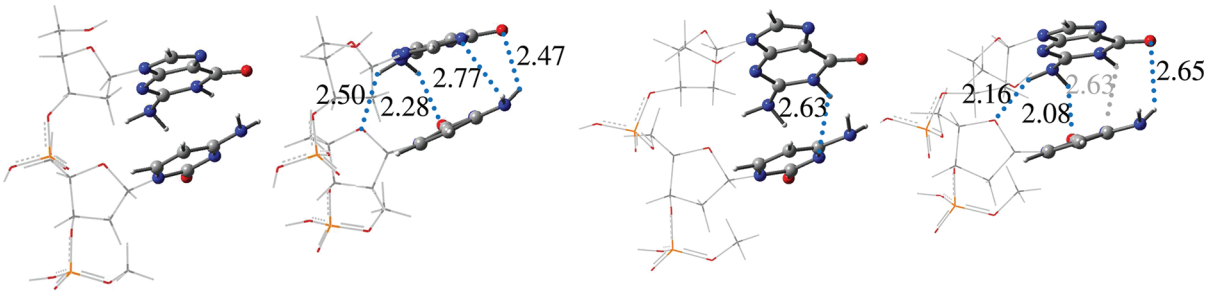

Figure 5. Two views of the optimized geometrical structures for dGpdCp and dGpdCp$^{\bullet-}$. Atomic distances are in Å. Color representations: orange for P, gray for C, red for O, blue for N, and white for H. Guanine in this dinucleoside corresponds to G−1 in dGpdCpdG.

the N1H1(G+1)N4(C) atomic angle of 150.3° suggest a strong H-bond. Since the cytosine is the proton acceptor in both H-bonds, these two strong H-bonds confirm formation of the cytosine-centered radical anion.

Interestingly, the base−base stacking is disrupted by the strengthened H-bonding interactions between G+1 and C in the radical anion of pdCpdG. The base−base angle in pdCpdG$^{\bullet-}$ amounts to 38.1°. Clearly, the base−base stacking is overtaken by the intrastrand H-bonding in pdCpdG$^{\bullet-}$.

It should be noted that the geometric parameters of pdCpdG are close to those predicted for the microhydrated dCpdG model in the previous study (with base−base distance of 3.53 Å and base−base angle of 22.5°).[36] However, the intrastrand H-bond N4(C)···H2(G) is 0.10 Å longer than that of pdGpdC, under the influence of the H-bonding network in the tetra-hydrated dCpdG. Moreover, the base−base stacking pattern in the microhydrated dCpdG radical anion[36] is less disturbed. This is due to the fact that the microhydration water molecules lock the neighboring G and C bases in the stacked form.

dGpdCp. The guanosine at the 3′ end of pdGpdCpdG is replaced by a methyl group in this model. The optimized structure of dGpdCp resembles the corresponding part in the oligomer of dGpdCpdG (Figure 5). The base−base distance is 3.21 Å and the base−base plane angle amounts to 10.5°, displaying the typical characteristics of the base−base stacking. Compared to the trimer, the intrastrand H-bonding between O6(G−1) and H4(C) is weakened in the dimer. The corresponding atomic distance is 2.47 Å and the atomic angle is 123.8° in dGpdCp. For comparison, in dGpdCpdG, these two values amount to 2.29 Å and 134.9°, respectively. On the other hand, H-bonds H2(G−1)···O2(C) and H′2(G−1)···O4′(C) in dGpdCp are similar to those in the trimer (the corresponding bond lengths: 2.28 Å vs 2.26 Å for H2(G−1)···O2(C) and 2.50 Å vs 2.54 Å for H′2(G−1)···O4′(C)). The stronger H-bonding between O6(G−1) and H4(C) in the trimer is a consequence of the existence of the H2(G+1)···N4(C) H-bond in which N4 of cytosine accepts the proton from the H2N2 moiety of G+1 and, therefore, improves the proton donating ability of the N4 site of C.

Electron attachment to dGpdCp improves the proton accepting capability and, thus, reinforces the H2(G−1)···O2(C) and H′2(G−1)···O4′(C) hydrogen bonds in dGpdCp$^{\bullet-}$. The corresponding H-bond lengths are 2.08 Å for H2(G−1)···O2(C) and 2.16 Å for H′2(G−1)···O4′(C) in the radical anion. The intrastrand interaction between O6(G−1) and H4(C) (if it exists) is very weak in the radical anion of the dimer, which corresponds to the atomic distance of 2.65 Å for O6(G−1) and H4(C) in dGpdCp$^{\bullet-}$. Accordingly, the attached electron is expected to be localized on the cytosine subunit.

The geometric parameters in Table 1 suggest that G−1 and C are moderately stacked in dGpdCp$^{\bullet-}$. The base−base distance of 3.46 Å and the base−base plane angle of 23.8° indicate that the base−base stacking pattern is somewhat disrupted by the negatively charged cytosine radical.

It is interesting that the base−base stacking structure of dGpdCp in neutral form is similar to the tetra-hydrated dGpdC.[36] However, the base−base distance in the radical anion of dGpdC is essentially the same as that in the neutral species. It could be concluded that the H-bonding networks through the microhydrated water molecules preserve the stacking pattern in the radical anion of dGpdC.

B. Electron Affinities and Energetic Properties. The significant positive electron affinities (Table 2) of dGpdCpdG suggest that the cytosine in the DNA single-strand represents a strong capturing site for excess electrons and is able to form an electronically stable radical anion center.

Table 2. Electron Affinities of Cytosine Containing Nucleic Acid Base, Nucleoside, Nucleotides, Oligonucleotides, and the Corresponding Micro-Hydrated Complexes (in eV)[a]

process	AEA	VEA[b]	VDE[c]
dGpdCpdG → dGpdCpdG$^{\bullet-}$	0.90	0.23	1.65
dGpdCp → dGpdCp$^{\bullet-}$	0.73	0.01	1.42
pdCpdG → pdCpdG$^{\bullet-}$	0.64	−0.12	1.41
dGpdC → [dGpdC] $^{\bullet-}$	0.64, *0.66*[d]	−0.11, *0.25*[d]	1.50, *1.42*[d]
dCpdG → [dCpdG] $^{\bullet-}$	0.90, *0.90*[d]	−0.17, *0.16*[d]	1.61, *1.64*[d]
3′,5′-dCDP → [3′,5′-dCDP]$^{\bullet-}$	0.24,[e] *0.27*[f]	−0.60,[e] *0.03*[f]	1.07,[e] *0.71*[f]
3′-dCMP → [3′-dCMP]$^{\bullet-}$	*0.33*[g]	*0.15*[g]	*1.28*[g]
dC → dC$^{\bullet-}$	*0.21*[h]	*−0.09*[h]	*0.72*[h]
C → C$^{\bullet-}$	−0.11,[d] *−0.09*[i]		
C1w → [C1w]$^{\bullet-}$	0.16(exptl),[j] *0.07−0.18*[k]		*0.15−0.93*[k]
C2w → [C2w]$^{\bullet-}$	0.29(exptl),[j] *0.03−0.41*[k]		*0.22−1.21*[k]

[a]Plain print is used for results obtained with the M05/DZP++, and *italics*, with B3LYP/DZP++. [b]VEA = E(neutral) − E(anion); the energies are evaluated using the optimized neutral structures. [c]VDE = E(neutral) − E(anion); the energies are evaluated using the optimized anion structures. [d]Reference 36, microhydrated with four water molecules. [e]Present work, with M05-2X/DZP++. [f]References 5 and 77. [g]References 4 and 34, where 3′-dCMP was labeled as 3′-dCMPH. [h]Reference 3. [i]References 3 and 30. [j]Reference 19. [k]Reference 59.

At the M05-2X/DZP++ level of theory, the adiabatic electron affinity of the dGpdCpdG nucleotide trimer is

dx.doi.org/10.1021/jp211386x | J. Phys. Chem. B 2012, 116, 1458−1466

predicted to be 0.90 eV. This value could be considered as analogous to the ultimate AEA value of cytosine in DNA single-strands in isolated form, since the model includes all the close neighboring constituents.

Compared to the AEA of dGpdCp (0.73 eV), an addition of a guanosine at the 3′ end (G+1) increases the AEA value of the trimer by about 0.17 eV. This increase could be attributed mainly to the effects of the intrastrand H-bond (H2(G+1)···N4(C)) brought by the G+1 fragment into the system. Both experimental and theoretical studies of the microhydrated cytosine conclude that each hydrating water molecule could raise the AEA of cytosine by about 0.13 eV.[19,59] On the other hand, introducing a guanosine at the 5′ end (G−1) enlarges the AEA of the system by about 0.26 eV (0.64 eV for pdCpdG vs 0.90 eV for dGpdCpdG). From the discussion of the geometric properties above, one can see that the addition of G−1 results in three more intrastrand H-bonds (H2(G−1)···O2(C), H′2(G−1)···O4′(C), and O6(G−1)···H4(C)). Therefore, it is the intrastrand H-bonding, rather than the base stacking, that governs the increase of the AEA of dGpdCpdG, as compared to that of the two dinucleosides.

It is important to note that in the radical anion of pdCpdG there is no base−base stacking interaction, while moderate base stacking is revealed in the radical anion of dGpdCp (based on the geometrical characteristics). The relatively large AEA for dGpdCp might be related to its base−base stacking pattern. However, one more H-bond in dGpdCp (as compared to pdCpdG) could also be the main reason for its relatively larger AEA (0.09 eV larger than that of pdCpdG). Combined with the discussion above, i.e., the conclusion that the intrastrand H-bonding governs the increase of the AEA, one can assume that the base stacking has little contribution to the electron capture capability of cytosine in DNA single strands. This is in agreement with the conclusion of the previous study of the microhydrated dGpdC models.[36]

Estimation of the vertical electron attachment energies (VEAs) is important for exploring the electron-capture behavior of DNA at the nascent stage of electron attachment. The substantial VEA predicted in the present investigation for the nucleotide trimer dGpdCpdG (0.23 eV) indicates that the cytosine- and guanine-rich DNA single strands are reasonable electron captors. In comparison, much smaller VEA values have been predicted by the M05-2X approach for the nucleotide dimers dGpdCp (0.01 eV) and pdCpdG (−0.12 eV). The increase in the VEA of dGpdCpdG suggests that the intrastrand interaction (intrastrand H-bonding and/or base−base stacking) from the neighboring guanosines is a critical factor for improving the effective electron capturing abilities of cytosine in DNA single strands. Notice that there is no intrastrand H-bonding interaction between C and G+1 in dGpdCpdG (the atomic distance of 2.61 Å between H2(G+1) and N4(C) in the neutral species indicates no H-bonding interaction). Therefore, the VEA difference (0.22 eV) between dGpdCpdG (VEA: 0.23 eV) and dGpdCp (VEA: 0.01 eV) should be the consequence of the base−base stacking between C and G+1. We conclude that the base−base stacking is important in enhancing the VEA, while it has less effect on the AEA.

The electronic stability of radical anions can be assessed by their vertical detachment energies (VDEs). VDE is the most commonly determined physical property in anion photodetachment experiments.[19,26,27] The VDE of the radical anion dGpdCpdG$^{\bullet-}$ has been predicted in order to evaluate its electronic stability. The VDE of dGpdCpdG$^{\bullet-}$ is 1.65 eV, about 0.23 eV larger than those for the single-stranded nucleotide dimers (1.42 eV for dGpdCp$^{\bullet-}$ and 1.41 eV for pdCpdG$^{\bullet-}$). Since C and G+1 do not adopt the stacking pattern in pdCpdG$^{\bullet-}$ while C and G−1 do assume the stacking pattern in dGpdCp$^{\bullet-}$, similar values of VDE for pdCpdG$^{\bullet-}$ and dGpdCp$^{\bullet-}$ imply that the base stacking has no effect on the VDE of the system. The VDE values of the studied models are far larger than the activation energy barriers needed for either N-glycosidic bond breaking or C′−O′ σ-bonds breaking in the cytosine centered radical anion of nucleotides.[1,4,76] These bond breakages should take place without causing the detachment of the excess electron from the cytosine centered radical anion of the single strand of DNA.

A polarizable medium has been found to have a profound effect on the studied phenomena. It enhances significantly the electron-capture ability of DNA segments. Using the polarizable continuum model (PCM), the AEA value for dGpdCpdG is estimated to be 2.06 eV. Under the analogous condition, the AEAs of dGpdCp and pdCpdG are evaluated to be 1.96 and 2.07 eV, respectively. It is important to note that the AEA values of forming the C-centered radical anions of DNA segments (ranging from nucleotide dCMP to dinucleotide dimer [dGpdC]$_2$)[4,5,34,36,60] are close to ∼2 eV in aqueous solutions (Table 3). Therefore, it is safe to assume that the ultimate value of the AEA of cytosine inside DNA in aqueous solutions is less than 2.50 eV. Moreover, the AEA values of pdCpdG and dGpdCpdG are so close that one concludes that stacking interactions between the bases should not increase the electron affinity of the system in the aqueous solutions.

Table 3. AEA of Cytosine Containing Nucleotides, Oligonucleotides, and Oligonucleotide Dimers in the Presence of Polarizable Medium (in eV)

process	AEA
dGpdCpdG → dGpdCpdG$^{\bullet-}$	2.06
dGpdCp → dGpdCp$^{\bullet-}$	1.96
pdCpdG → pdCpdG$^{\bullet-}$	2.07
[dGpdC]$_2$ → [dGpdC]$_2$ $^{\bullet-}$	2.03[a]
dGpdC → [dGpdC] $^{\bullet-}$	1.65[b]
dCpdG → [dCpdG] $^{\bullet-}$	1.91[b]
3′,5′-dCDP → [3′,5′-dCDP]$^{\bullet-}$	1.99[c]
3′-dCMP → [3′-dCMP]$^{\bullet-}$	1.89[d]

[a]Reference 60, microhydrated with eight water molecules. [b]Reference 36, microhydrated with four water molecules. [c]References 5 and 77. [d]References 4 and 34, where 3′-dCMP was labeled as 3′-dCMPH.

C. Charge Distributions and Molecular Orbital Analysis. The analysis of the distribution of negative charge on the constituent parts of the oligonucleotide provides insight into the overall electronic effect of the electron attachment. Table 4 summarizes the charge distributions among the bases, ribose, and phosphates for both the neutral and anionic complexes. The NPA charge differences between the neutral and anionic nucleotides support the conclusion that the attached electron mainly resides on the cytosine moieties in the dGpdCpdG$^{\bullet-}$ radical anion. The NPA charge differences reveal that there is 0.84 au of "extra negative charge" located on C and 0.06 e$^-$ of extra negative charge spreading over the ribose connected to cytosine. This observation is consistent with the character of the SOMO in Figure 6, where the unpaired electron is found mainly on the cytosine base with a small contribution extended to the connecting ribose. The negative

dx.doi.org/10.1021/jp211386x | J. Phys. Chem. B 2012, 116, 1458−1466

Table 4. NPA Charge Distributions of the Neutral and Radical Anion for dGpdCpdG

component	neutral	anion	Δ(A−N)[a]
C	−0.288	−1.123	−0.835
G−1	−0.258	−0.306	−0.048
G+1	−0.258	−0.273	−0.015
ribose (C)	1.017	0.957	−0.060
ribose (G−1)	0.959	0.956	−0.003
ribose (G+1)	0.967	0.957	−0.010
phosphate (5′C)	−0.769	−0.771	−0.002
phosphate (3′C)	−0.766	−0.787	−0.021
OH(5′)	−0.300	−0.297	0.003
OH(3′)	−0.305	−0.313	−0.008

[a]Δ(A−N): NPA charge difference between neutral and anionic species.

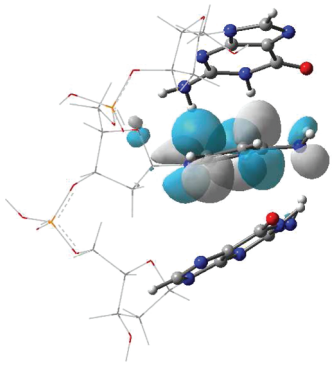

Figure 6. The singly occupied molecular orbital (SOMO) of $dGpdCpdG^{\bullet -}$.

charge on the ribose seems also to be extended to the O3′ atom that is directly linked to sugar ring, resulting in 0.02 e^- of extra negative charge spreading on the corresponding phosphate group. Meanwhile, since the O5′ atom connects to the sugar ring through the C5′ atom, less extra charge distribution is observed in the phosphate group attached to the 5′ position of cytidine. About 0.05 e^- of extra negative charge is found to reside on the guanine at the 5′ end (G−1). This part of the charge distribution should be transferred through the intrastrand H-bonds between G−1 and C. Comparatively, the negative charge distributed on G+1 amounts to only 0.02 au. Notice that the only intrastrand H-bonding between C and G +1 is through H2(G+1)···N4(C); the less negatively charged G +1unit suggests that the migration of the excess negative charge from C to G+1 should also proceed through this linkage.

The influence of the polarizable medium on the charge distributions of the neutral and radical anion of dGpdCpdG has also been studied by using the PCM model. The presence of the polarizable medium does not alter the charge distributions significantly for the studied systems (see Table S1 in the Supporting Information). The solvation only slightly increases the extra negative charge population on the cytosine moiety (by 0.014 au).

IV. CONCLUSIONS

The studied trimer of nucleotide dGpdCpdG is one of the simplest fragments of the DNA single stand that should be considered to be representative for the cytosine-centered DNA. Exploring electron attachment to this fundamental fragment of the DNA single strand enables one to approach reliable estimations of the electron accepting capabilities of a cytosine site in the DNA single strands.

For the first time, this smallest representative segment, dGpdCpdG, has been fully optimized and analyzed by a quantum mechanical approach at a reliable level of theory. The study of the electron attached dGpdCpdG demonstrates that cytosine contained DNA single strands have a strong tendency to capture low-energy electrons and to form electronically stable cytosine-centered radical anions. The relatively large vertical electron affinity and the significant adiabatic electron affinity predicted for the dGpdCpdG indicate that the cytosine bases are efficient electron captors in DNA single strands.

By comparative study of the model molecules pdCpdG and dGpdCp, one can conclude that base stacking has little contribution to the AEA of cytosine in the DNA single strands. Also, the base−base stacking does not affect the electronic stability of the cytosine-centered radicals. Intrastrand H-bonding is revealed to be critical in increasing the AEA and VDE of the cytosine-centered DNA fragments. However, base−base stacking is found to be important in enhancing the VEA of cytosine. The stacking between G and C increases the VEA of cytosine by about 0.2 eV. Therefore, base stacking should affect the initial stage of the electron capture process by increasing the probability of accepting electrons.

While the electron attachment to the cytosine moiety intensifies the intrastrand H-bonding between the neighboring G and C bases, it disrupts the base−base stacking interaction in the radical anion of dGpdCpdG.

The large VDE values of the studied models suggest that either N-glycosidic bond breaking or C′−O′ σ-bond breaking are capable occuring without causing the detachment of the unpaired electron from the cytosine centered radical anion of the single strand of DNA.

■ ASSOCIATED CONTENT

Supporting Information

Complete ref 73 and NPA charge distributions of the neutral and radical anion for dGpdCpdG in aqueous solutions (PCM model). This material is available free of charge via the Internet at http://pubs.acs.org.

■ AUTHOR INFORMATION

Corresponding Author

*E-mail: jiande@icnanotox.org (J.G.); jerzy@icnanotox.org (J.L.).

■ ACKNOWLEDGMENTS

Work in the USA was supported by the NSF CREST Grant No. HRD-0833178. In China, it was supported by National Science & Technology Major Project 'Key New Drug Creation and Manufacturing Program', China (Number: 2009ZX09301-001). We would like to thank the Mississippi Center for Supercomputing Research for a generous allotment of computer time.

■ REFERENCES

(1) Bao, X.; Wang, J.; Gu, J.; Leszczynski, J. *Proc. Natl. Acad. Sci. U.S.A.* **2006**, *103*, 5658−5663.

(2) Ray, S. G.; Daube, S. S.; Naaman, R. J. *Proc. Natl. Acad. Sci. U.S.A.* **2005**, *102*, 15−19.

(3) Richardson, N. A.; Gu, J.; Wang, S.; Xie, Y.; Schaefer, H. F. *J. Am. Chem. Soc.* **2004**, *126*, 4404−4411.

(4) Gu, J.; Wang, J.; Leszczynski, J. *J. Am. Chem. Soc.* **2006**, *128*, 9322−9323.
(5) Gu, J.; Xie, Y.; Schaefer, H. F. *Nucleic Acids Res.* **2007**, *35*, 5165−5172.
(6) Becker, D.; Sevilla, M. D. The Chemical Consequences of Radiation Damage to DNA. In *Advances in Radiation Biology*; Lett, J.; Academic Press: New York, 1993; Vol. *17*, pp 121−180.
(7) Kelley, S. O.; Barton, J. K. *Science* **1999**, *283*, 375−381.
(8) Ratner, M. *Nature* **1999**, *397*, 480−481.
(9) Boudaiffa, B.; Cloutier, P.; Hunting, D.; Huels, M. A.; Sanche, L. *Science* **2000**, *287*, 1658−1659.
(10) Pan, X.; Cloutier, P.; Hunting, D.; Sanche, L. *Phys. Rev. Lett.* **2003**, *90*, 208102.
(11) Caron, L. G.; Sanche, L. *Phys. Rev. Lett.* **2003**, *91*, 113201.
(12) Zheng, Y.; Cloutier, P.; Hunting, D.; Wagner, J. R.; Sanche, L. *J. Am. Chem. Soc.* **2004**, *126*, 1002−1003.
(13) Hall, D. B.; Holmlin, R. E.; Barton, J. K. *Nature* **1996**, *382*, 731−735.
(14) Steenken, S. *Biol. Chem.* **1997**, *378*, 1293−1297.
(15) Taubes, G. *Science* **1997**, *275*, 1420−1421.
(16) Berlin, Y. A.; Burin, A. L.; Ratner, M. A. *J. Am. Chem. Soc.* **2001**, *123*, 260−268.
(17) Beljonne, D.; Pourtois, G.; Ratner, M. A.; Bredas, J. L. *J. Am. Chem. Soc.* **2003**, *125*, 14510−14517.
(18) Huels, M. A.; Hahndorf, I.; Illenberger, E.; Sanche, L. *J. Chem. Phys.* **1998**, *108*, 1309−1312.
(19) Schiedt, J.; Weinkauf, R.; Neumark, D. M.; Schlag, E. W. *Chem. Phys.* **1998**, *239*, 511−524.
(20) Parsons, B. F.; Sheehan, S.; Yen, T. A.; Neumark, D. M.; Wehres, N.; Weinkauf, R. *Phys. Chem. Chem. Phys.* **2007**, *9*, 3291−3297.
(21) Desfrancois, D.; Abdoul-Carime, H.; Schermann, J. P. *J. Chem. Phys.* **1996**, *104*, 7792−7794.
(22) Periquet, V.; Moreau, A.; Carles, S.; Schermann, J. P.; Desfrancois, C. *J. Electron Spectrosc. Relat. Phenom.* **2000**, *106*, 141−151.
(23) Gutowski, M.; Dabkowska, I.; Rak, J.; Xu, S.; Nilles, J. M.; Radisic, D.; Bowen, K. H. *Eur. Phys. J. D* **2002**, *20*, 431−439.
(24) Haranczyk, M.; Gutowski, M.; Li, X.; Bowen, K. H. *Proc. Natl. Acad. Sci. U.S.A.* **2007**, *104*, 4804−4807.
(25) Haranczyk, M.; Gutowski, M.; Li, X.; Bowen, K. H. *J. Phys. Chem. B* **2007**, *111*, 14073−14076.
(26) Stokes, S. T.; Li, X.; Grubisic, A.; Ko, Y. J.; Bowen, K. H. *J. Chem. Phys.* **2007**, *127*, 084321.
(27) Radisic, D.; Bowen, K. H.; Dabkowska, I.; Storoniak, P.; Rak, J.; Gutowski, M. *J. Am. Chem. Soc.* **2005**, *127*, 6443−6450.
(28) Richardson, N. A.; Wesolowski, S. S.; Schaefer, H. F. *J. Phys. Chem. B* **2003**, *107*, 848−853.
(29) Haranczyk, M.; Gutowski, M. *Angew. Chem., Int. Ed.* **2005**, *44*, 6585−6588.
(30) Wesolowski, S. S.; Leininger, M. L.; Pentchev, P. N.; Schaefer, H. F. *J. Am. Chem. Soc.* **2001**, *123*, 4023−4028.
(31) Li, X.; Sevilla, M. D.; Sanche, L. *J. Am. Chem. Soc.* **2003**, *125*, 8916−8920.
(32) Ban, F.; Lundqvist, M. J.; Boyd, R. J.; Eriksson, L. A. *J. Am. Chem. Soc.* **2002**, *124*, 2753−2761.
(33) Rienstra-Kiracofe, J. C.; Tschumper, G. S.; Schaefer, H. F.; Nandi, S.; Ellison, G. B. *Chem. Rev.* **2002**, *102*, 231−282.
(34) Gu, J.; Xie, Y.; Schaefer, H. F. *J. Am. Chem. Soc.* **2006**, *128*, 1250−1252.
(35) Kumar, A.; Sevilla, M. D. *J. Phys. Chem. B* **2007**, *111*, 5464−5474.
(36) Gu, J.; Xie, Y.; Schaefer, H. F. *Chem.—Eur. J.* **2010**, *16*, 5089−5096.
(37) Gu, J.; Xie, Y.; Schaefer, H. F. *Chem. Phys. Lett.* **2009**, *473*, 213−219.
(38) Gu, J.; Xie, Y.; Schaefer, H. F. *J. Am. Chem. Soc.* **2005**, *127*, 1053−1057.
(39) Li, X.; Cai, Z.; Sevilla, M. D. *J. Phys. Chem. B* **2001**, *105*, 10115−10123.
(40) Li, X.; Cai, Z.; Sevilla, M. D. *J. Phys. Chem. A* **2002**, *106*, 9345−9351.
(41) Reynisson, J.; Steenken, S. *Phys. Chem. Chem .Phys.* **2002**, *4*, 5353−5358.
(42) Richardson, N. A.; Wesolowski, S. S.; Schaefer, H. F. *J. Am. Chem. Soc.* **2002**, *124*, 10163−10170.
(43) Gu, J.; Xie, Y.; Schaefer, H. F. *J. Phys. Chem. B* **2005**, *109*, 13067−13075.
(44) Gu, J.; Xie, Y.; Schaefer, H. F. *J. Chem. Phys.* **2007**, *127*, 155107.
(45) Kobylecka, M.; Jeszczynski, J.; Rak, J. *J. Am. Chem. Soc.* **2008**, *30*, 15683−15687.
(46) Gu, J.; Xie, Y.; Schaefer, H. F. *J. Phys. Chem. B* **2006**, *110*, 19696−19703.
(47) Smets, J.; McCarthy, W.; Adamowicz, L. *J. Phys. Chem.* **1996**, *100*, 14655−14660.
(48) Smets, J.; Smith, D. M. A.; Elkadi, Y.; Adamowicz, L. *J. Phys. Chem. A* **1997**, *101*, 9152−9156.
(49) Dologounitcheva, O.; Zakrzewski, V. G.; Ortiz, J. V. *J. Phys. Chem. A* **1999**, *103*, 7912−7917.
(50) Morgado, A.; Pichugin, K.; Adamowicz, L. *Phys. Chem. Chem. Phys.* **2004**, *6*, 2758−2762.
(51) Kumar, A.; Mishra, P. C.; Suhai, S. *J. Phys. Chem. A* **2005**, *109*, 3971−3979.
(52) Bao, X.; Sun, H.; Wong, N.; Gu, J. *J. Phys. Chem. B* **2006**, *110*, 5868−5874.
(53) Bao, X.; Liang, G.; Wong, N.; Gu, J. *J. Phys. Chem. A* **2007**, *111*, 666−672.
(54) Colson, A. O.; Besler, B.; Sevilla, M. D. *J. Phys. Chem.* **1993**, *97*, 13852−13859.
(55) Sevilla, M. D.; Besler, B. B.; Colson, A. O. *J. Phys. Chem.* **1994**, *98*, 2215.
(56) Hendricks, J. H.; Lyapustina, S. A.; de Clercq, H L.; Bowen, K. H. *J. Chem. Phys.* **1998**, *108*, 8−11.
(57) Kim, S.; Schaefer, H. F. *J. Chem. Phys.* **2006**, *125*, 144305.
(58) Kim, S.; Wheeler, S. E.; Schaefer, H. F. *J. Chem. Phys.* **2006**, *124*, 204310.
(59) Kim, S.; Schaefer, H. F. *J. Chem. Phys.* **2007**, *125*, 064301.
(60) Gu, J.; Wong, N.-B.; Xie, Y.; Schaefer, H. F. *Chem.—Eur. J.* **2010**, *16*, 13155−13162.
(61) Gu, J.; Xie, Y.; Schaefer, H. F. *ChemPhysChem* **2006**, *7*, 1885−1887.
(62) Lee, C.; Yang, W.; Parr, R. G. *Phys. Rev. B* **1988**, *37*, 785−789.
(63) Beck, A. D. *J. Chem. Phys.* **1993**, *98*, 1372−1377.
(64) Zhao, Y.; Truhlar, D. G. *Acc. Chem. Rev.* **2008**, *41*, 157−167.
(65) Zhao, Y.; Schultz, N. E.; Truhlar, D. G. *J. Chem. Theory Comput.* **2006**, *2*, 364−382.
(66) Gu, J.; Wang, J.; Leszczynski, J. *Chem. Phys. Lett.* **2011**, *512*, 108−112.
(67) Huzinaga, S. *J. Chem. Phys.* **1965**, *42*, 1293−1302.
(68) Dunning, T. H. *J. Chem. Phys.* **1970**, *53*, 2823−2833.
(69) Lee, T. J.; Schaefer, H. F. *J. Chem. Phys.* **1985**, *83*, 1784−1794.
(70) Reed, A. E.; Schleyer, P. R. *J. Am. Chem. Soc.* **1990**, *112*, 1434−1445.
(71) Reed, A. E.; Curtiss, L. A.; Weinhold, F. *Chem. Rev.* **1988**, *88*, 899−926.
(72) Cossi, M.; Barone, V.; Cammi, R.; Tomasi, J. *Chem. Phys. Lett.* **1996**, *255*, 327.
(73) Frisch, M. J.; Trucks, G. W.; Schlegel, H. B.; Scuseria, G. E.; Robb, M. A.; Cheeseman, J. R.; Montgomery, J. A., Jr.; Vreven, T.; Kudin, K. N.; Burant, J. C.et al. *Gaussian 03*, revision C.02; Gaussian, Inc.: Wallingford, CT, 2004.
(74) Sinden, R. R. *DNA Structure and Function*; Academic Press: New York, 1994.
(75) Jefferey, G. A.; Saenger, W. *Hydrogen Bonding in Bilogical Structures*; Springer-Verlag: New York, 1991.
(76) Gu, J.; Wang, J.; Leszczynski, J. *J. Am. Chem. Soc.* **2004**, *126*, 12651−12660.

(77) Gu, J.; Wang, J.; Leszczynski, J. *Nucleic Acids. Res.* **2010**, *38*, 5280−5290.